Isotype modulates epitope specificity, affinity, and antiviral activities of anti–HIV-1 human broadly neutralizing 2F5 antibody

Daniela Tudor[a,b,c], Huifeng Yu[a,b,c], Julien Maupetit[d,e], Anne-Sophie Drillet[a,b,c], Tahar Bouceba[f], Isabelle Schwartz-Cornil[a,b,c,1], Lucia Lopalco[g], Pierre Tuffery[d,e], and Morgane Bomsel[a,b,c,2]

[a]Mucosal Entry of HIV-1 and Mucosal Immunity, Cell Biology and Host–Pathogen Interactions Department, Cochin Institute, Centre National de la Recherche Scientifique Unité Mixte de Recherche 8104, 75014 Paris, France; [b]Université Paris Descartes, Sorbonne Paris Cité, 75014 Paris, France; [c]Institut National de la Santé et de la Recherche Médicale Unit 1016, 75014 Paris, France; [d]Molécules Thérapeutiques in Silico, Institut National de la Santé et de la Recherche Médicale Unité 973, Université Paris Diderot, Sorbonne Paris Cité 75205 Paris, France; [e]Ressource Parisienne en Bioinformatique Structurale, 75205 Paris, France; [f]Service Interactions des Biolmolécules, Institut de Biologie Intégrative IFR 83, Université Pierre et Marie Curie, 75013 Paris, France; and [g]San Raffaele Institute, 20127 Milan, Italy

Edited by Ian A. Wilson, The Scripps Research Institute, La Jolla, CA, and accepted by the Editorial Board May 21, 2012 (received for review January 19, 2012)

The constant heavy chain (CH1) domain affects antibody affinity and fine specificity, challenging the paradigm that only variable regions contribute to antigen binding. To investigate the role of the CH1 domain, we constructed IgA2 from the broadly neutralizing anti–HIV-1 2F5 IgG1, and compared 2F5 IgA2 and IgG binding affinity and functional activities. We found that 2F5 IgA2 bound to the gp41 membrane proximal external region with higher affinity than IgG1. Functionally, compared with IgG1, 2F5 IgA2 more efficiently blocked HIV-1 transcytosis across epithelial cells and $CD4^+$ cell infection by R5 HIV-1. The 2F5 IgG1 and IgA2 acted synergistically to fully block HIV-1 transfer from Langerhans to autologous $CD4^+$ T cells and to inhibit $CD4^+$ T-cell infection. Epitope mapping performed by screening a random peptide library and *in silico* docking modeling suggested that along with the 2F5 IgG canonical ELDKWA epitope on gp41, the IgG1 recognized an additional 3D-conformational epitope on the gp41 C-helix. In contrast, the IgA2 epitope included a unique conformational motif on the gp41 *N*-helix. Overall, the CH1 region of 2F5 contributes to shape its epitope specificity, antibody affinity, and functional activities. In the context of sexually transmitted infections such as HIV-1/AIDS, raising a mucosal IgA-based vaccine response should complement an IgG-based vaccine response in blocking HIV-1 transmission.

antibody structure | HIV-1 envelope gp41 | mucosa | mimotope

The ability of the constant heavy chain (CH1) domain to affect antibody affinity and fine specificity independent of avidity challenges the paradigm that only variable regions contribute to antigen binding (1). This suggests that the quality of the secondary/memory immune response, stronger or weaker, also may depend on the antibody isotype and must be taken into consideration in the vaccine design, especially for the mucosal pathogens like HIV-1.

A prophylactic vaccine against HIV-1 should focus on the induction of a protective immunity at mucosal surfaces involving HIV-1–specific IgAs and IgGs that can achieve different, but complementary, antiviral functions (2). Whereas IgG can induce efficient antibody-dependent cellular cytotoxicity (ADCC) (2–4), IgA blocks HIV transcytosis (5–7), and both can impede HIV-1 entry in dendritic cells or exert neutralizing activities against $CD4^+$ T-cell infection (8, 9). The role of gp41-specific IgAs in protecting against sexual transmission of HIV-1 in the absence of virus-specific IgGs has been demonstrated in vivo in highly HIV-1–exposed but persistently IgG-seronegative individuals (10, 11). Such IgAs could neutralize $CD4^+$ T-cell infection, and block HIV-1 transcytosis (7, 11, 12).

In humans, four main IgG isotypes occur—IgG1, IgG2, IgG3, and IgG4—differing in length and flexibility of the hinge region. In the case of HIV-1 infection, the dominant isotype is IgG1, although the broadly neutralizing IgG 2F5 was originally isolated as an IgG3 (13).

IgA exists as two subclasses, IgA1 and IgA2, found in similar amounts in the genital tract but not in the serum or the respiratory or upper intestinal tracts, where IgA1 largely dominates (14). Whereas in the cervical mucus IgA is rather polymeric, in the vagina equal proportions of monomeric and dimeric IgA are found (15). The two IgA subclasses appeared by gene duplication and thus share many similarities, the major difference being in the length of the hinge region, which accounts for their differing susceptibilities to proteases secreted by mucosal pathogens (14). Monomeric IgA2m(1), with a Fab-to-Fab distance of ∼8 nm, is more rigidly hinged and compact than monomeric IgA1, which has a Fab-to-Fab distance of 17 nm (14).

In earlier studies on the biological effect of constant heavy chain in HIV binding and neutralization, 2F5 IgG antibody together with 2G12, specific for HIV-1 envelope gp120, were class-switched from IgG1 to IgM and dimeric IgA1 (16). Compared with IgG1, dimeric-IgA1 2F5 displayed only poor activity in standard neutralization assay, but blocked up to 76% of viral transcytosis when applied at basal side of a tight epithelium, most likely in a pIg-R–mediated process (6). Recently, we showed that when applied at mucosal side, 2F5 IgG1 and dimeric-IgA1 had a similar, otherwise poor potential to block HIV-1 transcytosis across an epithelial monolayer, as well as HIV-1 entry into a rectal tissue (17). Similarly, switching the broadly neutralizing IgG1 b12, which is specific for gp120, to monomeric, dimeric, or polymeric IgA2s results in IgA with rather poor neutralizing activities against R5 and X4 tropic HIV-1 infection of $CD4^+$ cells, and with an equal potential, as IgG1, to block HIV-1 uptake by epithelial cells (18).

Finally, a panel of antibodies was created by switching the IgG2 human monoclonal antibody F425B4e8, specific for the base of the hypervariable V3 loop of the HIV-1 envelope gp120 (19). The resulting IgA1 captured significantly more virus than the corresponding IgG2, IgG3, and IgG1, but no statistical differences in the neutralization between various isotypes were observed (19).

In all of the foregoing studies, the respective role of each CH1 domain—gamma-1, alpha-1 or alpha-2—was not addressed. Our results in the present study demonstrate that the CH1 alpha-2

Author contributions: D.T. and M.B. designed research; D.T., H.Y., J.M., A.-S.D., T.B., I.S.-C., L.L., P.T., and M.B. performed research; D.T., H.Y., J.M., A.-S.D., T.B., I.S.-C., L.L., P.T., and M.B. analyzed data; and D.T. and M.B. wrote the paper.

The authors declare no conflict of interest.

This article is a PNAS Direct Submission. I.A.W. is a guest editor invited by the Editorial Board.

See Commentary on page 12272.

[1]Present address: Institut National de la Recherche Agronomique, Virologie et Immunologie Moléculaire, 78352 Jouy-en-Josas, France.

[2]To whom correspondence should be addressed. E-mail: morgane.bomsel@inserm.fr.

This article contains supporting information online at www.pnas.org/lookup/suppl/doi:10.1073/pnas.1200024109/-/DCSupplemental.

region clearly affects antibody fine specificity and affinity, as well as the extent of antiviral activities.

Results

2F5 IgA2 Has Greater Affinity than 2F5 IgG1 for the gp41 Membrane Proximal External Region and Captures the Free Virus More Efficiently. Functional monomeric 2F5 IgG1 and 2F5 IgA2 antibodies were produced in mammalian CHO cells, purified, and quantified by sandwich ELISA, as described in *Materials and Methods*. Binding of both 2F5 IgG1 and IgA2 to (*i*) ELDKWA, the nominal 2F5 IgG epitope (20); (*ii*) P1, the minimal membrane proximal external region (MPER) that allows for HIV-1 binding to galactosyl ceramide, the HIV-1 mucosal receptor (5, 9); and (*iii*) a trimeric recombinant gp41 protein (11) was comparatively evaluated by ELISA. $W_{666}A$ mutated P1 (5) was used as a negative control. Importantly, to preclude the possibility that the difference in binding to antigen was due to the detection antibody, anti-human heavy or kappa light chain was used.

Both 2F5 IgG1 and IgA2 specifically bound to P1 and ELDKWA in a dose-dependent manner (Fig. 1 *A* and *B*), but with greater efficiency for the IgA2. Thus, binding of 2F5 IgA2 at 0.1 nM to P1 and ELDKWA was equivalent to binding of 2F5 IgG1 and the reference 2F5 IgG1 (13) (2F5 IgG Pym) at 0.8 nM and 6.25 nM, respectively (Fig. 1*A*). Differences between isotypes were smaller, but still in favor of IgA2 when anti-kappa light chain was used for detection (Fig. 1*B*).

In addition, to confirm the enhanced binding of 2F5 IgA2 to ELDKWA, P1 and the rgp41, we tested this in a competition ELISA in the presence of an excess of 2F5 IgG1. An irrelevant human IgG was used as a control. We found that 25, 10, and 5 nM of 2F5 IgG1 were needed to compete with 0.027 nM of 2F5 IgA2 binding to ELDKWA, P1 (Fig. 1*C*), and rgp41 (Fig. 1*D*), respectively, and found no competition with the IgG (Fig. 1 *C* and *D*).

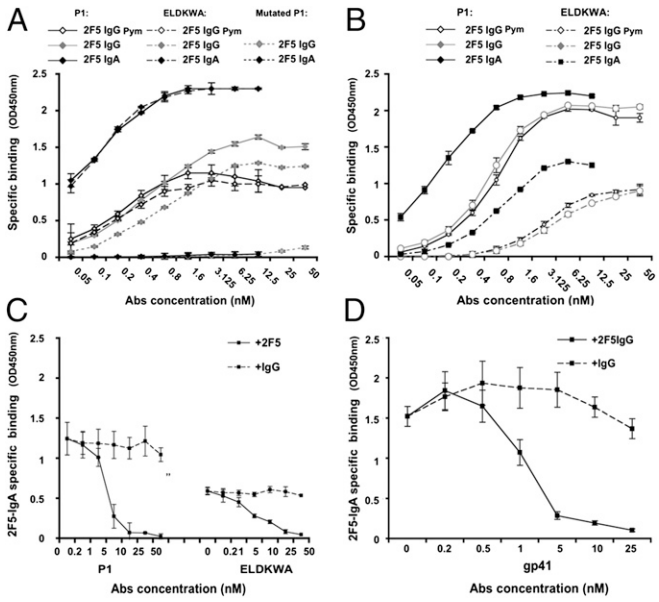

Fig. 1. The 2F5 IgA2 binds to gp41 MPER more robustly than 2F5 IgG1. 2F5 IgG1 and 2F5 IgA2 bind to P1, and ELDKWA in a dose-dependent manner. The specificity of 2F5 IgG1 (light gray) and of 2F5 IgA2 (black) for P1 (solid diamond, solid line) and for ELDKWA (solid diamond, broken line) was evaluated by ELISA. $W_{666}A$-mutated P1 (solid diamond, dotted line) served as a negative control. (*A* and *B*) Goat anti-human IgG or IgA (*A*) or mouse anti-human kappa light chain (*B*) were used as detection reagent to allow for direct comparison of both 2F5 isotypes. Specific binding (OD 450 nm) is plotted as a function of 2F5 Ab concentration (nM). (*C* and *D*) Competitive binding of 2F5 IgA2 to P1 and ELDKWA (*C*) or gp41 (*D*) in the presence of an excess of 2F5 IgG1 (solid diamond, solid line), or irrelevant IgG (solid diamond, dotted line) used as a negative control, was evaluated in competitive ELISA; 2F5 IgA2-specific binding (OD 450 nm) is plotted as function of the competitor IgG concentration (nM). Values in (*A–D*) represent mean ± SD of three independent experiments performed in duplicate.

Because the structure of P1 depends on lipids, we evaluated the affinities of 2F5 IgG1 and IgA2 on various P1-containing liposomes (21) (Table 1). The binding of both antibodies to P1-containing liposomes was one order of magnitude higher than the binding to P1 in solution; however, 2F5 IgA2 binding was 10-fold greater compared with IgG1, irrespective of the lipid context (Table 1). Similarly, 2F5 IgA2 binding for P1 alone was more than 10-fold greater than that of 2F5 IgG1 (with K_d = 0.2 and 7.3 nM, respectively; Table 1). Importantly, 2F5 IgG1 or IgA2 binding to liposome lacking P1 was less than twice the background binding obtained with an irrelevant IgG1 or IgA2 used as a negative control, indicating that in this setup, none of the 2F5 isotypes was cross-reactive (in agreement with ref. 22), and that an IgA2 switch does not provide cross-reactivity.

We next evaluated the affinity of the two 2F5 isotypes using surface plasmon resonance in kinetic experiments in which peptide P1 was immobilized, and 2F5 IgG1 and IgA2 at various concentrations were the analyte. The resulting affinity constant obtained for 2F5 IgG1 binding to peptide P1 is in good agreement with the literature (23–25). Importantly, the affinity of 2F5 IgA1 for peptide P1 was 30-fold greater than that of IgG1 counterpart, with K_d values of 0.29 nM for IgA2 and 11.1 nM for IgG1 (Fig. 2 *A* and *B*). These results confirm the differences in binding of 2F5 IgG1 and IgA2 for gp41 MPER found using ELISA approaches (Fig. 1 *A–D*).

Finally, considering the importance of the lipid environment in the affinities of 2F5 antibodies, and in an attempt to reproduce the in vivo conditions, we evaluated the ability of both 2F5 isotypes to bind the free virus. The results of virus capture ELISA showed that both 2F5 IgG1 and IgA2 isotypes specifically bound to R5 tropic HIV-1 JR-CSF, but with a significantly higher efficiency for 2F5 IgA2 than for IgG1 (Fig. 2*C*).

Taken together, these results indicate that 2F5 IgA2 bound to gp41 MPER and to free virus with higher affinity than IgG1. Given that 2F5 IgG1 and IgA2 have identical V regions and CL domain, these results suggest that some other regions of the antibody participate in antigen binding.

2F5 IgA2 and IgG1 Have Different Antiviral Efficiencies. We evaluated the functional activities of both isotypes using different in vitro experimental models that take into account the pathways of virus entry at the mucosal level.

2F5 IgA2 blocks HIV-1 transcytosis more efficiently than 2F5 IgG1. We first evaluated the potential of both isotypes to block the virus transcytosis, the pathway used by HIV-1 to penetrate across monostratified mucosal tissues (26). To do so, we conducted a comparative evaluation of transcytosis blockade by 2F5 IgA2 and IgG1

Table 1. Binding affinity of 2F5 IgA2 for gp41 MPER exceeds that of 2F5 IgG1

		K_d, nM	
		2F5 IgA2	2F5 IgG1
P1: lipids Molar ratio = 1:100	V1	0.024	0.31
	R1	0.05	0.50
	NR1	0.21	0.69
P1: lipids Molar ratio = 1:20	V2	0.024	0.41
	R2	0.061	0.61
	NR2	0.15	1.33
No lipid	P1	0.2	7.38

Binding affinities of 2F5 Abs to various P1-containing liposomes were measured by ELISA as described in *Materials and Methods*. NR, Phospholipid rich nonraft liposomes; R, glyco-sphingolipid rich raft liposomes; V, cholesterol and DHSM-rich, viral-like liposomes. Three analyses were performed independently and gave essentially the same results; results for only one of the analyses are shown.

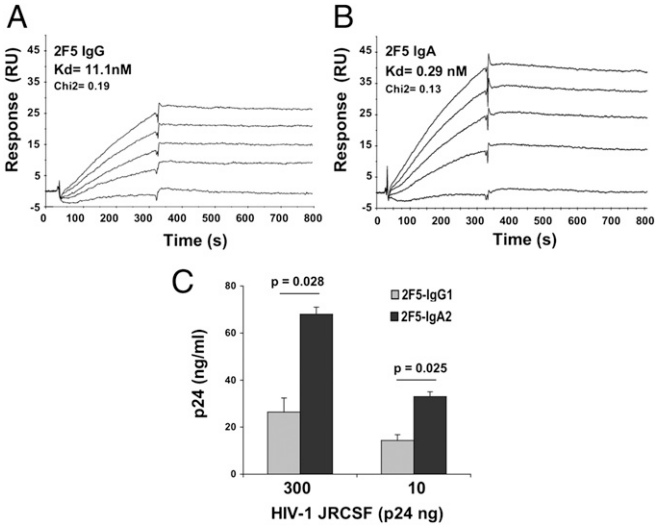

Fig. 2. The 2F5 IgA2 has greater affinity for gp41 MPER compared with 2F5 IgG1. P1 was immobilized on a CM-5 chip for surface plasmon resonance evaluation of an antibody affinity constant for P1. (*A* and *B*) 2F5 IgG1 (at 0, 0.1, 0.2, 0.3, and 0.4 nM) (*A*) and IgA2 (at 0, 0.5, 1, 1.5, and 2 nM) (*B*) were the analytes. The K_d and corresponding Pearson's χ^2 test (Chi2) values shown were estimated by global curve fitting of the specific binding responses. Fitted curves are in black. Injections were carried out in duplicate and gave essentially the same results. Only one of the duplicates is shown. (*C*) 2F5 IgA2- and IgG1-specific binding to HIV-1 JR-CSF virions. 2F5 IgG1 (gray bars) or IgA2 (black bars) bound to goat anti-human IgG- or IgA-coated ELISA plates were incubated with HIV-1 JR-CSF for 1 h at 37 °C. HIV-1 binding was evaluated by measuring the p24 content after removal of unbound virus. Results are presented as HIV-1 p24 captured by 2F5 IgA2 or IgG1 after subtraction of the nonspecific binding (HIV-1 p24 captured by irrelevant IgA2 or IgG). Values represent mean ± SD of two independent experiments performed in triplicate.

of cell free HIV-1, or initiated on contact with HIV-1–infected peripheral blood mononuclear cells (PBMCs). Both 2F5 antibodies blocked virus transcytosis, but in a more robust manner for the IgA2 compared with the IgG1 (IC_{90} = 1 nM for IgA2 and 10 nM for IgG1) (Fig. 3*A*). In addition, cell-free HIV transcytosis, although 100-fold less efficient than when induced from HIV-1–infected cells (27), was also better blocked by 2F5 IgA2 than by IgG1, as we reported previously (17).

2F5 IgG1 and IgA2 act synergistically to block HIV-1 transfer from Langerhans cells to T cells. We further evaluated how 2F5 IgG1 and IgA2 blocked the virus transfer from Langerhans (LC) to T cells (one of the ways that HIV-1 penetrates via pluristratified epithelia; ref. 28). We found that 2F5, not as IgG1 or as IgA2, at 17 or 66 nM, was able to efficiently block HIV-1 transfer to autologous $CD4^+$ T lymphocytes (although a limited, 30% block was found for IgG1 at 66 nM) (Fig. 3*B*). Interestingly, combining both isotypes in equal proportion to reach 33 nM or 66 nM completely inhibited the virus transfer from LCs to $CD4^+$ T lymphocytes (Fig. 3*B*), suggesting that the isotypes could act synergistically.

2F5 IgA2 neutralizes $CD4^+$ T-cell infection by R5 tropic HIV-1 better than 2F5 IgG1. We further evaluated the potential of 2F5 IgA2 and IgG1 to neutralize the $CD4^+$ T cell HIV-1 infection on $CD4^+$ cells, either primary T lymphocytes or CEM-$CD4^+CXCR4^+CCR5^+$ cells (CEM-$CCR5^+$), which provides a more reproducible and precise test for evaluation of neutralization (29). Both isotypes equally neutralized (without statistically significant differences) the infection of $CD4^+$ T lymphocytes in a dose-dependent manner (Fig. 3*C*). Here again, a robust neutralization was obtained when the two isotypes were combined in equally low concentrations, to reach 0.033 nM, suggesting a synergistic effect (Fig. 3*C*).

Both 2F5 antibody isotypes also neutralized infection of CEM-$CCR5^+$ target cells in a dose-dependent manner (Fig. 3*D*). Importantly, 2F5 IgA2 neutralized infection more robustly than 2F5 IgG1, with a 20-fold lower IC_{99} (P = 0.005), a 10-fold lower IC_{90} (P = 0.006), and a 33-fold lower IC_{50} (P = 0.004) (Fig. 3*D*).

Finally, we compared neutralization activities of the two 2F5 isotypes in the TZM-bl cell assay against the pseudoviruses expressing the HIV-1 QH0692.42 envelope (2). In this assay, again IC_{90} and IC_{50} were lower for 2F5 IgA2 compared with 2F5 IgG1 (Table 2).

Taken together, the findings from this set of functional tests demonstrate that 2F5 IgA2 and IgG1 have different efficiencies of antiviral activities in vitro. Importantly, combining both isotypes resulted in a synergistic effect on neutralization of the $CD4^+$ T lymphocytes, albeit to a restricted panel of R5 tropic HIV-1 strain, and completely blocked virus transfer from LCs to autologous $CD4^+$ T cells.

2F5 IgA2 and IgG1 Epitopes Map to Different Discontinuous Sequences on gp41. Although both 2F5 isotypes bound to the 2F5 IgG1 canonical epitope ELDKWA (Fig. 1), the differences in antiviral activities suggested that each antibody could recognize larger but different 3D epitopes. Therefore, using phage display (30, 31), we screened on 2F5 IgA2 or IgG1 a random peptide library expressed on M13 phages, to comparatively determine the specific sequences able to bind each antibody isotype. Such specific sequences correspond to the antibody epitope (referred to as mimotope). For each antibody, this screening resulted in the selection of 100 clones that match 22 and 25 different sequences lacking internal gaps, the latter usually corresponding to ambiguously sequenced residues (Fig. 4).

We investigated the existence of a conserved linear motif in each set of specific sequences compared with the gp41 C-helix region by multiple alignment with the T-Coffee algorithm (32), which applies triplet library extensions (as detailed in *Materials and Methods*). Sequences screened on 2F5 IgG1 and Ig2A shared a well-conserved motif centered around DRW and DKW, as expected (13, 33). For IgG1, six different sequences were selected with an occurrence ≥3. For 2F5 IgA2, six selected sequences also were retrieved with an occurrence ≥3, including one sequence with a frequency of 7 and another with a frequency of 11. Similarities within IgA2-selected peptides and the gp41 C-helix sequence taken together were longer, namely DRWA and DKWA, as described initially for the 2F5 IgG1 (13). Importantly, the more reliable color index for the IgA2 was correlated with its higher binding efficiency for ELDKWA compared with the IgG1 (Fig. 1). However, for both isotypes, terminal parts of selected sequences, representing >60% of the full peptide amino acids (3 or 4 over the total of 12 amino acids), could not be mapped to the gp41 C-helix. This suggests that both antibodies recognize a conformational binding site apart from the gp41 canonical motif ELDKWA. Therefore, we used *in silico* component approaches to identify their respective conformational 3D epitopes.

Along with the 2F5 IgG Epitope on the MPER, 2F5 IgG1 Binds to Another C-Helix Epitope, Whereas IgA2 Binds to the *N*-Helix of gp41. Recently developed software allows for 3D analysis of epitopes. Thus, *in silico* approaches [e.g., Mapitope (34), Pepitope (35), 3DEX (30)] map 3D epitopes on the surface of a protein structure obtained by crystallography, by using algorithms that take into account the relative distance and physicochemical properties of individual amino acids. A discontinuous 3D epitope is localized on the protein surface by searching for a 3D fit with partial amino acid strings of a given sequence in a preset distance. This algorithm is repeated for each string of amino acids until the full peptide sequence is analyzed.

We used the sole published crystallographic structure of gp41 encompassing its entire hydrophobic MPER as a template. This structure most likely represents the six-helix bundle configuration composed of three *N*-helices and three C-helices working during HIV fusion with target cells (36), although such a close proximity between the C-helix and the *N*-helix also exists in the structure of the gp41 spike on free virus (37, 38).

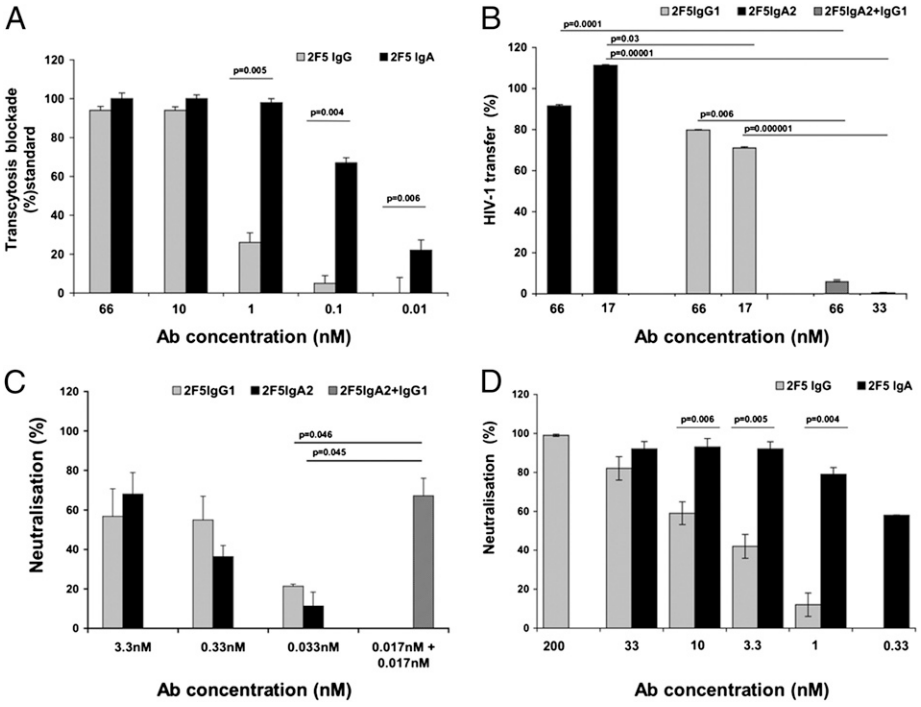

Fig. 3. The 2F5 IgA2 and IgG1 have different anti-viral efficiencies. (*A*) Transcytosis of HIV-1, induced by HIV-1 R5-infected PBMCs, across epithelial cells for 2 h was measured after pre-incubation of HIV$^+$ PBMCs with 2F5 IgG1 (gray bars) or IgA2 (black bars). Results are presented as percentage of transcytosis blockade in the absence of Abs. (*B*) Inhibition of HIV-1 transfer from LCs to autologous CD4$^+$ T cells evaluated by measuring the p24 released by LCs / T cells cocultures at day 5. HIV-1 JR-CSF was pre-incubated with LCs for 2 h before addition of the antibodies, either alone (2F5 IgG1, gray bars; 2F5 IgA2, black bars) or in combination (hatched bars), and T cells. Results are presented as percentage of transfer inhibition in the absence of Abs. (*C* and *D*) Dose-dependent inhibition of HIV-1 neutralization mediated by 2F5 Abs assessed in a single cycle infectivity assay, using p24 staining on primary CD4$^+$ T cells (*C*) and CEM-CCR5$^+$ cell line (*D*); 2F5 IgG1 (gray bars), IgA2 (black bars), or their combination (hatched bars), were incubated for 1 h at 37 °C with HIV-1JR-CSF before the addition of CD4$^+$ cells for 36 h. The percentage of neutralization was defined as the reduction of p24$^+$ cells compared with control-infected cells in the absence of Abs. Values represent mean ± SD of at least three independent experiments performed in duplicate for *A* and *B* and in triplicate for *C* and *D*.

Localization of selected sequences on gp41 six-helix bundle structure, using the Pepitope method, is shown in Fig. 5. For each gp41 chain, the frequency of the residues predicted to belong to an epitope is plotted along the protein sequence. Using this algorithm, we found that, in addition to binding to ELDKWA on gp41 C-helix, a second motif located on the same helix, namely NYTSLIHSLI, could be recognized by 2F5 IgG1 (Fig. 5 *A* and *B*). Pepitope analysis also suggested that residues of the gp41 *N*-helix in the vicinity of the C-helix ELDKWA motif, namely ASMTLTVQAR, also could be involved in the motif recognized by the 2F5 IgA2, suggesting a larger conformational 3D epitope (Fig. 5 *C* and *D*). The normalized Pepitope score allows for better evaluation of the efficiency of antibody binding to gp41. Strikingly, the score associated to the cluster NYTSLIHSLI recognized by 2F5 IgG1 (19.647) was much lower than that associated with the second cluster ASMTLTVQAR recognized by IgA2 (261.52).

These results clearly suggest that 2F5 IgG1 and IgA2 may recognize extra motifs in addition to the canonical ELDKWA potentially forming conformational 3D motifs. This correlates with the observed biological properties of the two isotypes.

Discussion

This study aimed to assess the influence of antibody isotype including that of the CH1 region, on antibody affinity, epitope specificity, and neutralizing activity. Thus, we comparatively evaluated a set of recombinant human IgG1 and IgA2 that carries the H and L chain variable domains of the broadly neutralizing HIV-1 gp41-specific Ab 2F5. The specific antiviral activities reported for each antibody isotype and their synergy may apply to the protection against HIV-1 infection at the mucosal level.

We have focused on the monomeric IgA2, because (*i*) it is less susceptible to degradation compared with IgA1 (14); (*ii*) 2F5 was previously switched to a dimeric IgA1, with no improvement in binding efficiency compared with the IgG1 (16); and (*iii*) 2F5 dimeric IgA1 is less potent than monomeric IgA2 in blocking HIV transcytosis across rectal tissue (17). We show that monomeric 2F5 IgA2 bound to gp41 MPER and free virus with greater efficiency than IgG1.

The avidity parameter cannot explain the differences between the 2F5 IgG1 and IgA2 isotypes, because both are monomeric. Furthermore, the low density of the envelope spike trimer at the HIV-1 surface, with interspike distance too far apart for a bivalent antibody to bridge, precludes any influence of avidity on antibody antiviral activities (39).

Antibody affinity results from the process of affinity maturation occurring at the level of the variable complementary determining region loops and, particularly for HIV-1– specific antibodies, at the level of framework loops (11, 40). However, the CH1-domain can provide additional structural constraints that participate in the antibody structure and paratope conformation (41), modulating the specificity and affinity.

Here we have provided evidence on the impact of the CH1 region on antibody fine specificity, corresponding to differences in antigen binding by antibodies with the same CL, VL, and VH regions. The entire CH region could well participate to the differences in the 2F5 affinity for gp41 MPER. Rather, it is the amount and distribution of electrostatic and hydrophobic interactions present within CH1 domain of either 2F5 IgA2 or IgG1 (differing by 70% in sequence) that would allow the antigen-binding site to establish stronger or weaker interactions with the antigen.

Our *in silico* analyses have identified potential conformational 3D epitopes specific for each 2F5 isotype. Thus, molecular modeling of the mimotopes on the gp41 surface indicated that W666 and Lys665 from the ELDKWA epitope tightly interacted with the 2F5 IgA2 paratope, as demonstrated by a highly reliable CORE index (Figs. 4 and 5), in agreement with its higher affinity for P1

Table 2. 2F5 IgA2 has greater potential than 2F5 IgG1 to neutralize TZM-bl cell infection by R5 tropic HIV-1

Ab	Ab concentration, ng/mL	
	IC_{50}	IC_{90}
2F5 IgA2	0.32 ± 0.05	1.06 ± 0.12
2F5 IgG1	2.56 ± 0.35	>6.67

Neutralization of envelope pseudotyped HIV-1 R5 tropic QH0692.42 infection mediated by 2F5 Abs was evaluated using the TZM-bl assay. The antibody concentrations causing 50% (IC_{50}) and 90% (IC_{90}) reductions in luciferase reporter gene production were determined by regression analysis.

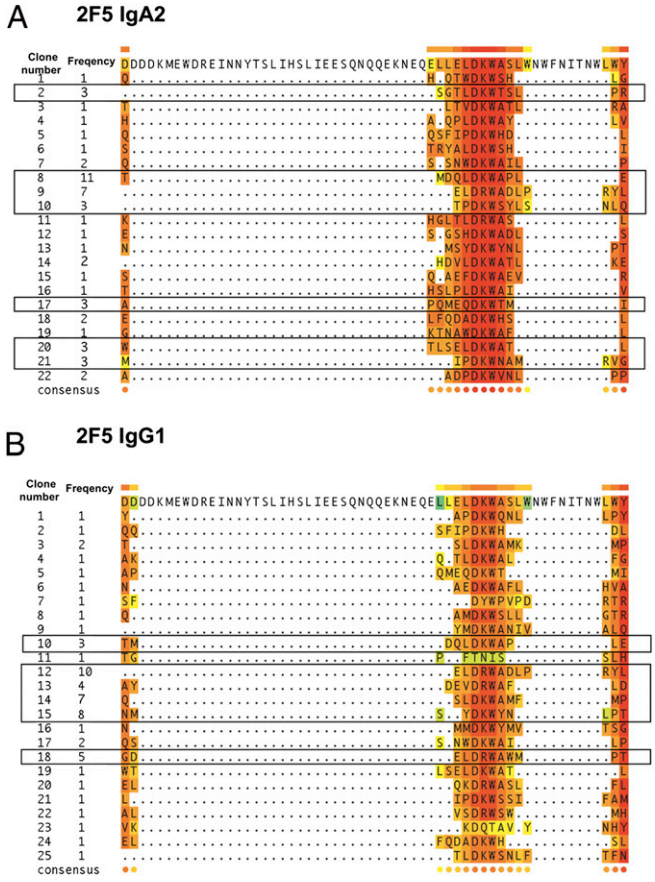

Fig. 4. Multiple alignment of sequences specific for gp 41 and 2F5 IgG1 or IgA2. Sequences of epitopes retrieved after panning the random 12-mer library on 2F5 IgA2 (*A*) or IgG1 (*B*) used for *in silico* analyses. The multiple alignment on selected sequences together with the gp41 C-helix sequence was performed with the T-Coffee server (32). Frequency refers to the retrieval occurrence obtained for each sequence. Specific sequences retrieved with a frequency of ≥3 are framed. Each residue is colored following the T-Coffee conservation color scheme (CORE), ranging from blue (low conservation) to red (high conservation). The last line in each panel (consensus sequence) highlights amino acids feature conservation, along the reference gp41 sequence, following the same color code.

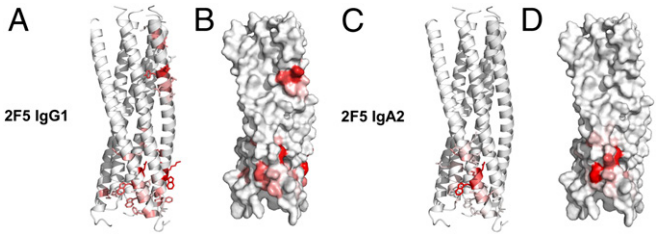

Fig. 5. Both 2F5 IgA2 and IgG1 recognize different nonlinear epitopes on gp41 when organized as a six-helix bundle. 2F5IgG1-predicted (*A* and *B*) and IgA2-predicted (*C* and *D*) epitope amino acid frequencies are mapped using a red gradient (the more red, the higher the frequency) onto the gp41 structure (36), represented as a ribbon diagram (*A* and *C*) or molecular surface (*B* and *D*).

(Figs. 1 and 2). Moreover, 2F5 IgA2 possibly could interact not only with the expected 2F5 epitope (LDKWA) located on gp41 C-helix, but also with an additional region in the spatial vicinity of ELDKWA on the adjacent gp41 *N*-helix (ASMTLTVQAR), defining a larger 3D conformational binding site. In contrast, 2F5 IgG1 interacts with a different epitope (NYTSLIHSLI) located on the N-terminal of the C-helix, at a distance of ~30 nm, that most likely preclude binding of the two motifs by the two Fab sites of a single IgG1 molecule (39).

Considering the sequence from the adjacent gp41 *N*-helix as being part of the 2F5 IgA2 epitope, its higher affinity could be rationalized as follows: 2F5 IgA2 may first bind to the gp41 *N*-helix, allowing antibody anchoring for subsequent conformational adjustment after this initial encounter, thereby favoring the tighter interactions with W666 and the Lys665. Alternatively, 2F5 IgA2 may first bind to the gp41 C-helix, and the strong interaction with the W666 and the Lys665 could consequently hinder binding to the ASMTLTVQAR sequence situated in close spatial proximity.

In agreement with the present data, recombinant IgA and IgG1 anti-tubulin antibody engineered from the same V regions have shown significant differences in affinity, in favor of IgA (42, 43). Such differences also have been observed at the monovalent Fab level (42). Therefore, the CH1 domain appears to play a role in modulating antibody affinity as a consequence of the greater CH1 alpha flexibility, which confers to the IgA a higher kinetically competent form to bind the antigen (42, 43). Similar results also have been obtained for different IgG isotypes and relative Fabs to *Cryptococcus neoformans* with identical V regions (41). Moreover, in our own previous studies, gp41-specific Fabs of IgAs from HIV-1–exposed but persistently IgG-seronegative individuals exhibited higher affinity for gp41 compared with IgG (11).

In addition to differences in the affinity of 2F5 IgA2 and IgG1 isotypes, our present results suggest the 3D complexity of the 2F5 epitope, confirming earlier studies extending the ELDKWA epitope to the linear sequence NEQELLELDKWASLWN (44). This 3D epitope differs between 2F5 IgG1 and IgA2 isotypes, and possibly could account for the differences in their biological properties. Thus, the unique 3D epitope specific for 2F5 IgA2 is most likely exposed during the prefusion conformation of an HIV envelope spike, namely before virus binding to epithelial cells or during transcytosis, a process that does not require a change in HIV envelope spike conformation. Binding of IgA2, but not of IgG1, to that epitope could increase the transcytosis blocking efficiency of IgA2. In contrast, the additional epitope recognized by 2F5 IgG1 on the N-terminal part of the gp41 C-helix is more accessible when the virus spike changes conformation to achieve fusion with $CD4^+$ T cells (45). This possibly could account for the synergy of 2F5 IgA2 and IgG1; 2F5 IgA2 could better bind the virion before it interacts with the LCs, as was also shown by virus capture ELISA and ELISA with P1 presented on liposomes (Fig. 2*C* and Table 1), whereas the 2F5 IgG1 also could bind gp41 in the fusion state using the NYTSLIHSLI epitope that is better exposed. Consequently, the virus binding by both isotypes drives an enhancement of $CD4^+$ T-cell neutralization, or completely blocks the virus transfer. Synergy between IgG1 and IgA2 could apply in the submucosa, where both isotypes may be produced locally (2, 46).

HIV-1 is transmitted mainly at mucosal sites through several pathways, including transcytosis and uptake by dendritic cells, LCs, and intraepithelial $CD4^+$ T cells (28). We have shown that 2F5 antibodies could interfere with the initial steps of HIV-1 mucosal transmission in either monostratified or multilayered epithelia, before virus dissemination. Both isotypes blocked HIV-1 transcytosis in agreement with our previous study on rectal tissue (17), reduced the infection of $CD4^+$ T cells by CCR5-tropic and clade B R5 tropic HIV-1, and diminished HIV-1 transfer from LCs to autologous $CD4^+$ T cells. However, 2F5 IgA2 was more efficient in blocking virus transcytosis and inhibiting $CD4^+$ cell infection, whereas 2F5 IgG1 was superior in blocking HIV-1 transfer from LCs to $CD4^+$ T cells. Finally, 2F5 IgA2 and IgG1 were seen to act synergistically in blocking HIV-1 transfer from LCs to autologous T cells and in reducing $CD4^+$ T-cell infection.

In conclusion, the enhanced affinity of 2F5 IgA2 for gp41 MPER provides important evidence supporting a dominant role

of the antibody CH1 region in modulating antibody affinity and fine specificity and can further explain the differences in antiviral activity between 2F5 IgA2 and IgG1. Furthermore, our results indicate that both isotypes IgG1 and IgA2 of 2F5 Ab interfere in vitro with the earliest steps of HIV-1 transmission across mucosal surfaces, suggesting that in vivo IgA and IgG antibodies could have complementary and synergistic antiviral activities. Thus, the design of effective anti-HIV vaccines should focus on induction of both IgA and IgG antibodies on this major portal of entry for HIV-1.

Materials and Methods

For 2F5 IgG1, DNA of 2F5 V regions was cloned into VHExpress and VKExpress, which direct the synthesis of human γ-1 heavy chain and light chain synthesis, respectively. Alternatively, 2F5 IgG1 was obtained from Polymun. For the 2F5 IgA2, the same DNA V regions were cloned into the pcDNA3:VHCα2m(1) and pcDNA3:VLCκ. Vectors were expressed in CHO *dhfr*$^-$ cells for monomeric 2F5 IgA2 and IgG1 production. IgA2 purification was performed using the CaptureSelect human IgA affinity matrix (BAC) and 2F5 IgG1 by protein A chromatography in accordance with the manufacturer's instructions.

ELISA was performed as described previously (3, 11). Functional assays where performed following our previously established methods for transcytosis of TZM-bl cells with envelope-pseudotyped viruses, and single-cycle neutralization assays as described previously (11). Inhibition of HIV-1 transfer from LCs to T cells was assessed using a modified method (9) by adding appropriate antibody after virus uptake by LCs. Surface plasmon resonance experiments were performed as described previously (25) with a Biacore 3000 instrument. P1 peptide was immobilized on CM5 chips (GE Healthcare), and the antibodies were the analyte for the kinetic measurements. Epitope mapping was performed as described previously (30). Bioinformatics analyses were performed essentially using Pepitope software (http://pepitope.tau.ac.il) and the trimeric gp41 structure (36). More detailed information is available in *SI Materials and Methods*.

ACKNOWLEDGMENTS. We thank Dr. Blaise Corthesy (Swiss Institute for Experimental Cancer Research, Lausanne, Switzerland) for kindly providing IgA2 expression vectors, the Pepitope authors for their constructive feedback, and Dr. Olga Starodub for the English editing.

1. Torres M, Casadevall A (2008) The immunoglobulin constant region contributes to affinity and specificity. *Trends Immunol* 29:91–97.
2. Bomsel M, et al. (2011) Immunization with HIV-1 gp41 subunit virosomes induces mucosal antibodies protecting nonhuman primates against vaginal SHIV challenges. *Immunity* 34:269–280.
3. Tudor D, Bomsel M (2011) The broadly neutralizing HIV-1 IgG 2F5 elicits gp41-specific antibody-dependent cell cytotoxicity in a FcγRI-dependent manner. *AIDS* 25:751–759.
4. Klein JS, Webster A, Gnanapragasam PN, Galimidi RP, Bjorkman PJ (2010) A dimeric form of the HIV-1 antibody 2G12 elicits potent antibody-dependent cellular cytotoxicity. *AIDS* 24:1633–1640.
5. Alfsen A, Iniguez P, Bouguyon E, Bomsel M (2001) Secretory IgA specific for a conserved epitope on gp41 envelope glycoprotein inhibits epithelial transcytosis of HIV-1. *J Immunol* 166:6257–6265.
6. Bomsel M, et al. (1998) Intracellular neutralization of HIV transcytosis across tight epithelial barriers by anti-HIV envelope protein dIgA or IgM. *Immunity* 9:277–287.
7. Miyazawa M, et al.; ESN Study Group(2009) The "immunologic advantage" of HIV-exposed seronegative individuals. *AIDS* 23:161–175.
8. Ganesh L, et al. (2004) Infection of specific dendritic cells by CCR5-tropic human immunodeficiency virus type 1 promotes cell-mediated transmission of virus resistant to broadly neutralizing antibodies. *J Virol* 78:11980–11987.
9. Magérus-Chatinet A, et al. (2007) Galactosyl ceramide expressed on dendritic cells can mediate HIV-1 transfer from monocyte derived dendritic cells to autologous T cells. *Virology* 362:67–74.
10. Mazzoli S, et al. (1997) HIV-specific mucosal and cellular immunity in HIV-seronegative partners of HIV-seropositive individuals. *Nat Med* 3:1250–1257.
11. Tudor D, et al. (2009) HIV-1 gp41-specific monoclonal mucosal IgAs derived from highly exposed but IgG-seronegative individuals block HIV-1 epithelial transcytosis and neutralize CD4(+) cell infection: An IgA gene and functional analysis. *Mucosal Immunol* 2:412–426.
12. Devito C, et al. (2002) Cross-clade HIV-1–specific neutralizing IgA in mucosal and systemic compartments of HIV-1–exposed, persistently seronegative subjects. *J Acquir Immune Defic Syndr* 30:413–420.
13. Purtscher M, et al. (1994) A broadly neutralizing human monoclonal antibody against gp41 of human immunodeficiency virus type 1. *AIDS Res Hum Retroviruses* 10:1651–1658.
14. Furtado PB, et al. (2004) Solution structure determination of monomeric human IgA2 by X-ray and neutron scattering, analytical ultracentrifugation and constrained modelling: A comparison with monomeric human IgA1. *J Mol Biol* 338:921–941.
15. Johansson M, Lycke NY (2003) Immunology of the human genital tract. *Curr Opin Infect Dis* 16:43–49.
16. Wolbank S, Kunert R, Stiegler G, Katinger H (2003) Characterization of human class-switched polymeric (immunoglobulin M [IgM] and IgA) anti-human immunodeficiency virus type 1 antibodies 2F5 and 2G12. *J Virol* 77:4095–4103.
17. Shen R, et al. (2010) GP41-specific antibody blocks cell-free HIV type 1 transcytosis through human rectal mucosa and model colonic epithelium. *J Immunol* 184:3648–3655.
18. Mantis NJ, et al. (2007) Inhibition of HIV-1 infectivity and epithelial cell transfer by human monoclonal IgG and IgA antibodies carrying the b12 V region. *J Immunol* 179:3144–3152.
19. Liu F, et al. (2003) Expression and functional activity of isotype and subclass switched human monoclonal antibody reactive with the base of the V3 loop of HIV-1 gp120. *AIDS Res Hum Retroviruses* 19:597–607.
20. Purtscher M, et al. (1996) Restricted antigenic variability of the epitope recognized by the neutralizing gp41 antibody 2F5. *AIDS* 10:587–593.
21. Coutant J, et al. (2008) Both lipid environment and pH are critical for determining physiological solution structure of 3D-conserved epitopes of the HIV-1 gp41-MPER peptide P1. *FASEB J* 22:4338–4351.
22. Scherer EM, Zwick MB, Teyton L, Burton DR (2007) Difficulties in eliciting broadly neutralizing anti-HIV antibodies are not explained by cardiolipin autoreactivity. *AIDS* 21:2131–2139.
23. Shen X, et al. (2010) Prolonged exposure of the HIV-1 gp41 membrane proximal region with L669S substitution. *Proc Natl Acad Sci USA* 107:5972–5977.
24. Zhang MY, et al. (2008) Cross-reactive human immunodeficiency virus type 1-neutralizing human monoclonal antibody that recognizes a novel conformational epitope on gp41 and lacks reactivity against self-antigens. *J Virol* 82:6869–6879.
25. Frey G, et al. (2008) A fusion-intermediate state of HIV-1 gp41 targeted by broadly neutralizing antibodies. *Proc Natl Acad Sci USA* 105:3739–3744.
26. Bomsel M (1997) Transcytosis of infectious human immunodeficiency virus across a tight human epithelial cell line barrier. *Nat Med* 3:42–47.
27. Alfsen A, Yu H, Magérus-Chatinet A, Schmitt A, Bomsel M (2005) HIV-1–infected blood mononuclear cells form an integrin- and agrin-dependent viral synapse to induce efficient HIV-1 transcytosis across epithelial cell monolayer. *Mol Biol Cell* 16:4267–4279.
28. Hladik F, Hope TJ (2009) HIV infection of the genital mucosa in women. *Curr HIV/AIDS Rep* 6:20–28.
29. Trkola A, Matthews J, Gordon C, Ketas T, Moore JP (1999) A cell line-based neutralization assay for primary human immunodeficiency virus type 1 isolates that use either the CCR5 or the CXCR4 coreceptor. *J Virol* 73:8966–8974.
30. Humbert M, et al. (2008) Inducing cross-clade neutralizing antibodies against HIV-1 by immunofocusing. *PLoS ONE* 3:e3937.
31. Saphire EO, et al. (2007) Structure of a high-affinity "mimotope" peptide bound to HIV-1–neutralizing antibody b12 explains its inability to elicit gp120 cross-reactive antibodies. *J Mol Biol* 369:696–709.
32. Di Tommaso P, et al. (2011) T-Coffee: A Web server for the multiple sequence alignment of protein and RNA sequences using structural information and homology extension. *Nucleic Acids Res* 39(Web server issue):W13-7.
33. Zwick MB, et al. (2005) Anti-human immunodeficiency virus type 1 (HIV-1) antibodies 2F5 and 4E10 require surprisingly few crucial residues in the membrane-proximal external region of glycoprotein gp41 to neutralize HIV-1. *J Virol* 79:1252–1261.
34. Bublil EM, et al. (2007) Stepwise prediction of conformational discontinuous B-cell epitopes using the Mapitope algorithm. *Proteins* 68:294–304.
35. Mayrose I, et al. (2007) Epitope mapping using combinatorial phage-display libraries: A graph-based algorithm. *Nucleic Acids Res* 35:69–78.
36. Buzon V, et al. (2010) Crystal structure of HIV-1 gp41 including both fusion peptide and membrane proximal external regions. *PLoS Pathog* 6:e1000880.
37. Roux KH, Taylor KA (2007) AIDS virus envelope spike structure. *Curr Opin Struct Biol* 17:244–252.
38. White TA, et al. (2010) Molecular architectures of trimeric SIV and HIV-1 envelope glycoproteins on intact viruses: Strain-dependent variation in quaternary structure. *PLoS Pathog* 6:e1001249.
39. Klein JS, Bjorkman PJ (2010) Few and far between: How HIV may be evading antibody avidity. *PLoS Pathog* 6:e1000908.
40. Zwick MB, et al. (2003) Molecular features of the broadly neutralizing immunoglobulin G1 b12 required for recognition of human immunodeficiency virus type 1 gp120. *J Virol* 77:5863–5876.
41. Torres M, Fernández-Fuentes N, Fiser A, Casadevall A (2007) The immunoglobulin heavy chain constant region affects kinetic and thermodynamic parameters of antibody variable region interactions with antigen. *J Biol Chem* 282:13917–13927.
42. Pritsch O, et al. (1996) Can immunoglobulin C(H)1 constant region domain modulate antigen binding affinity of antibodies? *J Clin Invest* 98:2235–2243.
43. Pritsch O, et al. (2000) Can isotype switch modulate antigen-binding affinity and influence clonal selection? *Eur J Immunol* 30:3387–3395.
44. Parker CE, et al. (2001) Fine definition of the epitope on the gp41 glycoprotein of human immunodeficiency virus type 1 for the neutralizing monoclonal antibody 2F5. *J Virol* 75:10906–10911.
45. Chan DC, Kim PS (1998) HIV entry and its inhibition. *Cell* 93:681–684.
46. Brandtzaeg P (2009) Mucosal immunity: Induction, dissemination, and effector functions. *Scand J Immunol* 70:505–515.